DOI: 10.1002/eji.201747260 Eur. J. Immunol. 2018. 48: 430–440

Basic

European Journal of Immunology

Adaptive immunity

Research Article

"Double-duty" conventional dendritic cells in the amphibian *Xenopus* as the prototype for antigen presentation to B cells

Harold R. Neely[1,2], Jacqueline Guo[1], Emily M. Flowers[1], Michael F. Criscitiello[3] and Martin F. Flajnik[1]

[1] Department of Microbiology and Immunology, University of Maryland Baltimore, Baltimore, MD, USA
[2] Department of Microbiology and Immunobiology, Harvard Medical School, Boston, MA, USA
[3] Vet. Med. and Biomedical Sciences, Texas A&M University, College Station, TX, USA

Two populations of dendritic cells (DCs) are found in mammals, one derived from hematopoietic precursors (conventional/cDC), and another derived from mesenchymal precursors, the follicular DC (FDC); the latter is specialized for antigen presentation to B cells, and has only been definitively demonstrated in mammals. Both cDC and FDC are necessary for induction of germinal centers (GC) and GC-dependent class switch recombination (CSR) and somatic hypermutation (SHM). We demonstrate that in *Xenopus*, an amphibian in which immunoglobulin CSR and SHM occur without GC formation, a single type of DC has properties of both cDC and FDC, including high expression of MHC class II for the former and display of native antigen at the cell surface for the latter. Our data confirm that the advent of FDC functionality preceded emergence of bona fide FDC, which was in turn crucial for the development of GC formation and efficient affinity maturation in mammals.

Keywords: Antigen handling · Dendritic cell · Evolution · Fc-Receptor · Follicular dendritic cell


See accompanying commentary by Robert


Additional supporting information may be found in the online version of this article at the publisher's web-site

Introduction

Together with the antigen receptors (immunoglobulins (Ig) and T cell receptors (TCR)) and the major histocompatibility complex (MHC), secondary lymphoid organs (SLO) emerged at the inception of adaptive immunity in jawed vertebrates [1, 2]. The spleen was the first SLO to emerge in the evolution of jawed vertebrates, and a distinction of T and B cell zones, or at least specific cellular concentrations of T and B cells, is found in almost every species examined [2]. As defined in mammals, antigen presenting cells (APCs) are an essential component of adaptive responses, presenting foreign antigen to both B and T cells. T cells recognize antigens in the form of peptides bound to MHC class I and class II molecules on hematopoietically derived dendritic cells (DCs) that migrate into T cell zones upon encountering antigen. B cells, in stark contrast, recognize conformational determinants on antigen presented as immune complexes on the surface of follicular DC (FDC), which are sessile cells derived from perivascular mural cells during mammalian embryogenesis. FDC are also required

Correspondence: Dr. Martin F. Flajnik
e-mail: mflajnik@som.umaryland.edu

for maintenance of B cell follicles (FO), and follicular migration away from the central arteriole during embryogenesis, as well as selection of antigen-specific B cells both for primary responses and (especially) during germinal center formation [3].

APC with the ultrastructure of DC have been detected in all jawed vertebrates [4]. In the adult *Xenopus* spleen, the B cell follicle retains the embryonic condition of remaining associated with the vasculature, and it is surrounded by a two-cell layer of elongated cells termed the Grenzschichtmembran of Sterba (GS) [5]; T cells surround the follicle as a loosely defined zone [6]. A single, morphologically homogeneous population of DC has been described in the *Xenopus* spleen. These cells, termed XL cells, were originally described as "large, mitotically active cells with abundant electron lucent cytoplasm, large hyperlobulated nuclei and prominent nucleoli . . . found in the periphery of the splenic white pulp" [7]. Additionally, these DC were shown to be distinct from macrophages by demonstrating a lack of staining for non-specific esterase and only a minimal capacity to phagocytose colloidal carbon [8], and distinct from B cells by an absence of intracellular Ig. XL cells migrate into the white pulp (WP) in the context of acute, thymus-dependent immune responses, predominantly localizing to the internal perimeter of the WP, and seem to be capable of trapping Ag at their plasma membrane [5, 7].

Based on these observations, and a gestalt view of DC evolution in gnathostomes, we hypothesized that the *Xenopus* XL cells are of a conventional, hematopoietic lineage (cDC), but perform "double duty," presenting both peptide:MHC Ag to T cells, and native, surface-bound Ag to B cells. Here, we confirm the previous identification of the XL cells, and establish a method of readily identifying and isolating them. Further, we provide a detailed analysis of XL cell behavior, sub-splenic localization, expression of molecules at the cell surface, and transcriptional profile during acute immune responses. We propose that our data are compatible with a combined phenotype of cDC/FDC in all ectothermic vertebrates (indeed, the capacity of mammalian cDC to retain/present native Ag has been demonstrated [9–11], and these studies may have revealed the primitive functions of cDC) and provide new hypotheses for the differentiation/function of such 'double duty' DC. Our data suggest that the capacity of cDC to adsorb and present native Ag predates the emergence of bona fide FDC, and further that the emergence of FDC in warm-blooded vertebrates, *not* SHM or CSR, was likely the major advance required for GC formation and advanced affinity maturation of humoral immunity.

Results

XL cells in the WP of naïve and immunized Xenopus adults

As in all characterized jawed vertebrates [12–14], the onset of WP ontogeny in the *Xenopus* spleen is marked by an accumulation of surface IgM-positive B cells around splenic vasculature, forming a follicle by two weeks post-fertilization (Fig. 1A). The microarchitecture of the mature, adult *Xenopus* WP is characterized by retention of the embryonic feature of B cell follicles around the vasculature [6] (Fig. 1B), bounded by the F-actin-rich GS (visualized with Phalloidin, Supporting Information Fig. 1). Few T cells are observed in the WP of a quiescent *Xenopus* spleen; rather, they reside in a corona surrounding and peripheral to the WP [15]. Of note, numbers of T cells surrounding a given WP vary from a single layer of cells adjacent to the GS to larger, sometimes asymmetric populations. This microarchitectural organization is in stark contrast with the mature mammalian WP; during mammalian WP ontogeny, the nascent B cell FO is rapidly replaced at the vasculature by the T cell peri-arteriolar lymphoid sheath (PALS) [12]. This migration is dependent upon the lymphotoxin (LT) $\alpha 1\beta 2$-dependent maturation of perivascular pre-FDC into FDC, and their concurrent detachment and co-migration with the nascent FO from the vasculature [16]. With this in mind, the retention of the mature B cell FO around the splenic vasculature suggests a lack of bona fide FDC in *Xenopus*. Furthermore, ultrastructural analyses of the *Xenopus* WP, and WP of all other examined amphibians and fish, have not revealed cells with the morphological characteristics of FDC, and GC do not form in the *Xenopus* WP [17]. Our new data, and all previous studies in the field of comparative immunology, argue against the presence of bona fide FDC in the *Xenopus* spleen and likely in all ectothermic vertebrates.

As mentioned, only a single, morphologically homogeneous population of DC – distinct from macrophages -termed XL cells- has been described in the *Xenopus* spleen. XL cells, which represent approximately 3% of total splenocytes [5], are large cells with high cytoplasmic content, multi-lobed nuclei, and dendritic processes – all characteristics of DC (Fig. 1C). In the steady-state, XL cells are distributed throughout both the red pulp (RP) and WP. In the context of an acute, thymus-dependent immune response, XL cells have been shown to migrate across the GS into the WP [7, 18], and within 7 days of immunization (50 ug hen egg lysozyme (HEL) in CFA), we indeed observed a repositioning of XL cells at the internal perimeter of the WP, forming a very well-defined ring just inside the GS (Supporting Information Fig. 2C).

Antigen (Ag) trafficking into the WP of the *Xenopus* spleen has been reported [5]. Immunizing Ag was shown to localize to the internal perimeter of the WP, in a pattern later shown to be consistent with the repositioned XL cells; this led to the prediction that XL cells are responsible for Ag trafficking into the WP [7]. Of note, this Ag trafficking into the WP was shown to be T cell-dependent – no immunogen was detectable in either the WP or the RP of thymectomized animals, as we have confirmed here ([19] Supporting Information Fig. 3A). We observed no conspicuous changes in the WP of thymectomized animals, as has been reported [18]. As with the positioning of the B cell FO relative to the vasculature, this mode of Ag trafficking contrasts with that seen in mammals. Transport of Ag into the mammalian FO (either in the splenic WP or the lymph node) is predominantly mediated in a T cell-independent manner by complement receptor- (CR-) mediated "handoff" of immune complexes from macrophages to B cells, and subsequently from B cells to FDC, the latter of which are already positioned within and throughout the FO.

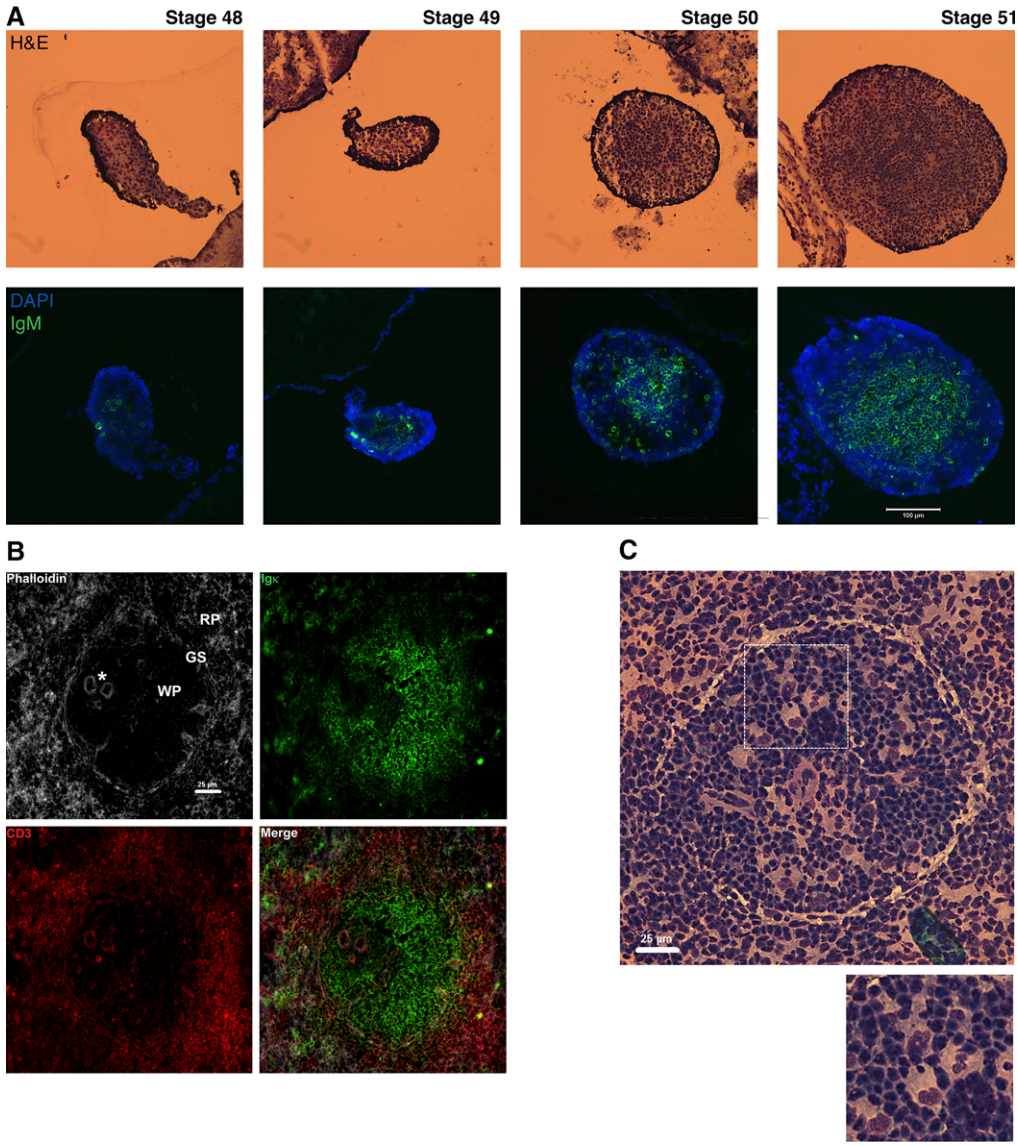

Figure 1. Microarchitecture of the *Xenopus* WP in naïve animals. (A) (*Upper row*) Representative cryosection images of larval *Xenopus* spleen at indicated developmental stages, stained with H&E. (*Lower row*) cryosections, adjacent to above sections, stained with mAb anti-IgM (green) and DAPI (blue). Data are representative of at least three independent experiments with 3 samples per experiment, with 3 animals per developmental timepoint. Magnification 200×, scale bar: 100 μm. (B) Cryosection of a single, representative adult *Xenopus* splenic WP from a quiescent animal, stained with Phalloidin (white), mAb Igk-specific (green), and pAb CD3-specific (red). RP: red pulp, WP: white pulp, GS, Grenzschichtmembran of Sterba. Asterisk indicates central vasculature in the Phalloidin stain. (C) Cryosection of a single, representative adult WP from a quiescent animal, stained with H&E. Boxed area enlarged to show individual XL cell morphology. (B and C) Data are representative of at least 3 independent experiments with 5 animals. Magnification 200×, scale bars: 25 μm.

XL cells as FDC

In order to determine whether the Ag previously reported at the internal perimeter of the WP is indeed XL cell-associated, we immunized animals with R-Phycoerythrin (PE) in incomplete Freund's Adjuvant (IFA). As with HEL, we observed a repositioning of XL cells to the internal perimeter of the WP, forming an organized ring inside the GS (Fig. 2A). We chose the fluorochrome PE as our immunogen in order to evaluate acquisition and retention of native Ag [20, 21] internalization and proteolytic degradation of PE will result in an abolition of its fluorescence. Thus, cell-associated PE fluorescence is indicative of acquisition and retention of immunogen in its native form. Overlay of PE fluorescence onto H&E-stained cryosections revealed colocalization of immunogen with the repositioned XL cells within the WP, demonstrating both acquisition and retention of native Ag by XL cells. Of note, by day 9 post-immunization, PE was detected at the internal perimeter of every splenic WP (Fig. 2B), and was only very rarely detected in the RP. Furthermore, accumulation of PE in the WP was not observed prior to 7 days post-immunization (Supporting

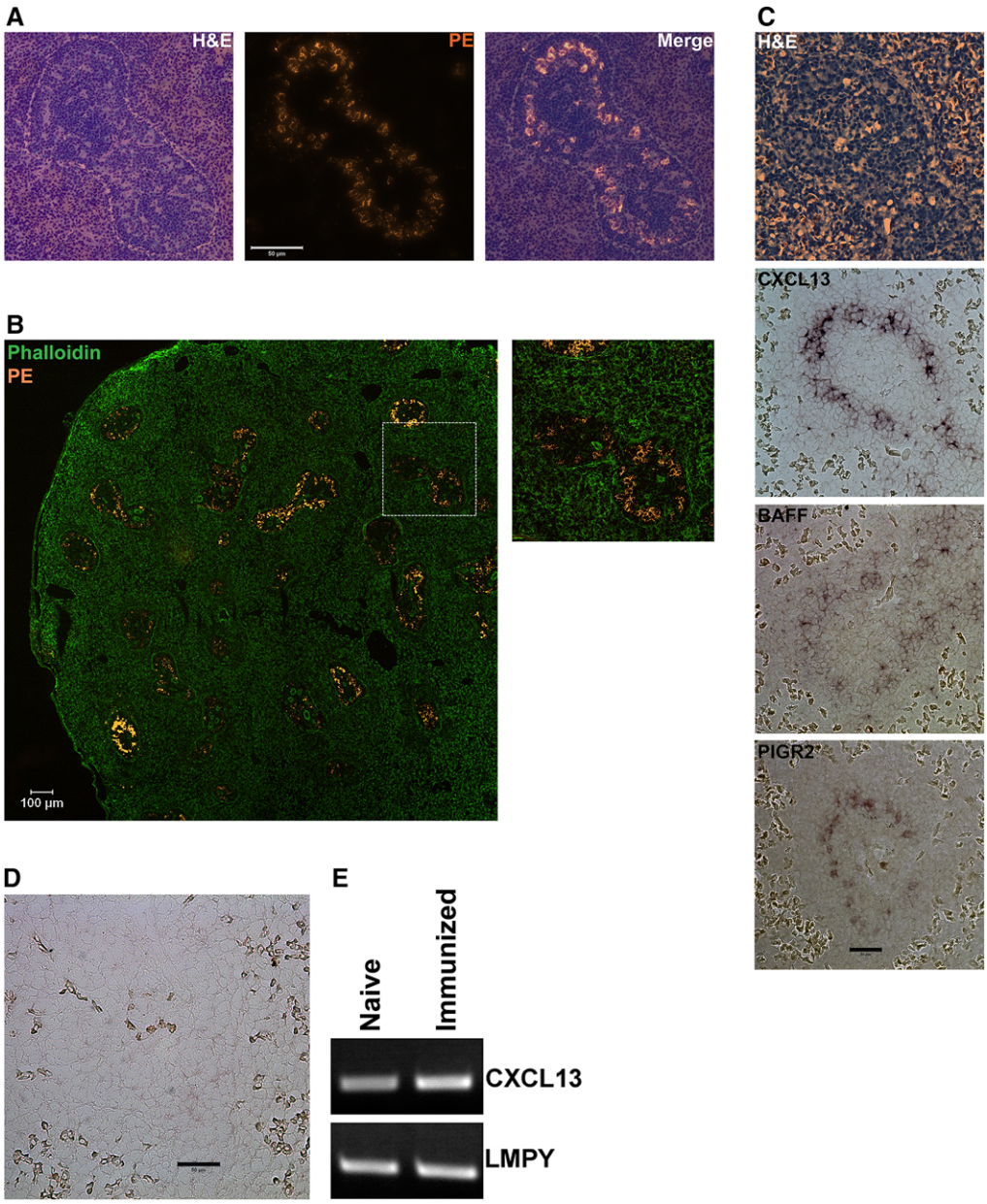

Figure 2. Antigen handling and induction of gene expression by XL cells in the immunized *Xenopus* spleen. (A) Fluorescent and histological analysis of a representative cryosection from day 9 post-immunization (PE/IFA) spleen. Section was imaged for PE fluorescence (*center panel*) and subsequently stained with H&E (*left panel*), and images were manually overlaid (*right panel*). Data are representative of 3 independent experiments with 1 Xenopus per experiment and 3 animals in total. Magnification 200×, scale bar: 50 μm. (B) Fluorescent analysis of a representative day 9 post-immunization spleen, stained with Phalloidin (green) and imaged for PE fluorescence (orange). Data are representative of 3 independent experiments with 1–2 animals per experiment, 5 animals in total. Magnification 40×, scale bar: 100 μm. (C) ISH analysis of cryosections from day 9 post-immunization spleen. Sections were probed as noted on the figure for CXCL13, BAFF, and PIGR2. (D) ISH analysis of a representative cryosection from quiescent spleen, probed for CXCL13. (D and E) Data are representative of at least three independent experiments with 1 animal per experiment, each for naïve and immunized. Magnification 400×, scale bars: 50 μm. (E) Semi-quantitative RT-PCR analysis of Cxcl13 mRNA expression in quiescent and day 9 post-immunization spleen, versus housekeeping gene LMPY. Data are representative of 3 independent experiments on RNA extracted from 1 naïve and 1 immunized spleen per experiment, 3 animals each condition in total.

Information Fig. 2B), suggesting an active trafficking of Ag into the WP rather than passive accumulation mediated by natural IgM immune complexes (IC). To address the possibility of internalization of PE without degradation and therefore confirm surface retention of immunogen, we immunized animals with unlabeled goat IgG and were able to detect surface retention by FACS using a fluorescently labeled donkey anti-goat IgG (not shown).

Surface retention of native Ag by XL cells is a hallmark of FDC function in mammals. We therefore analyzed splenic cryosections

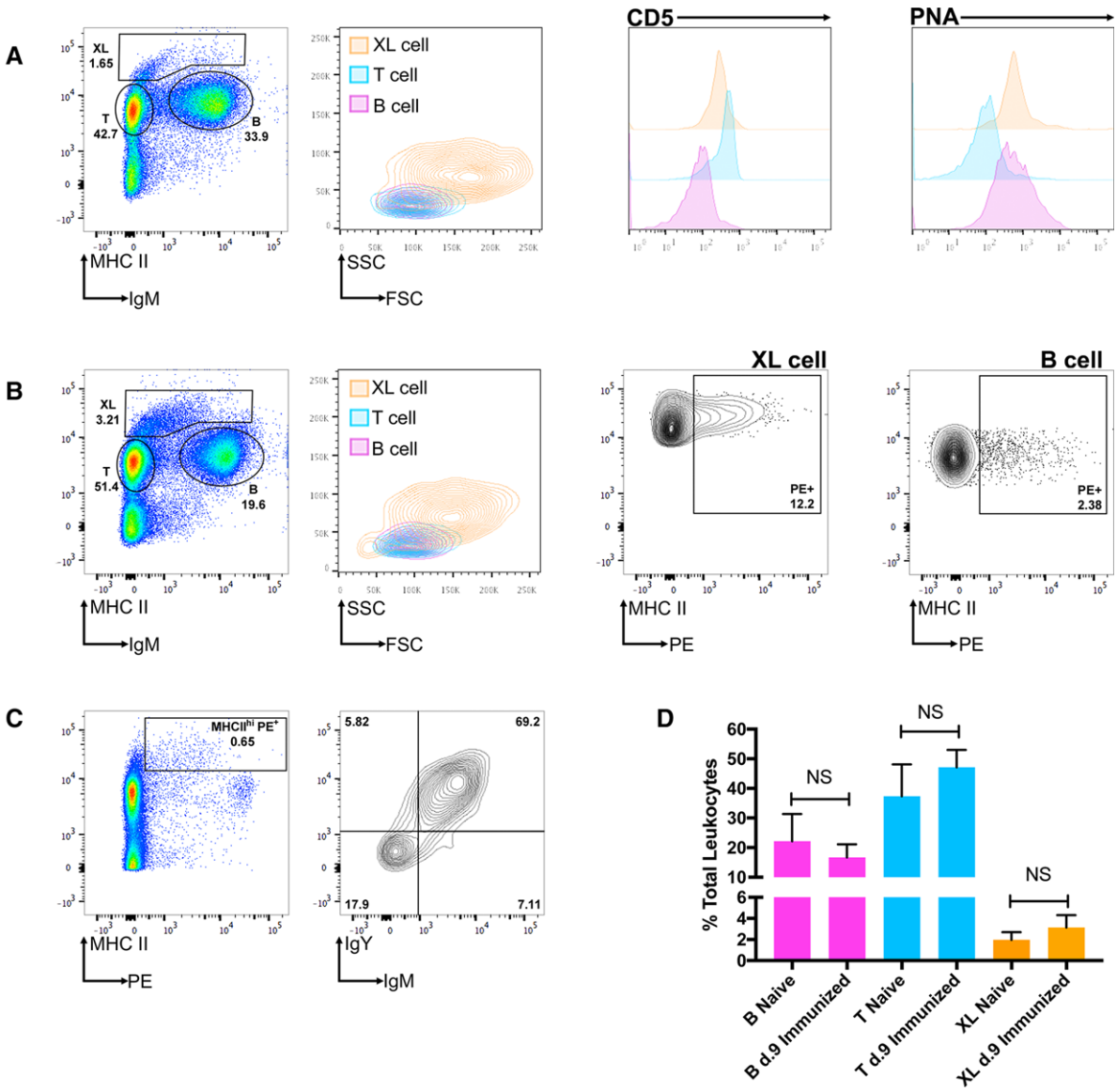

Figure 3. XL cells are MHC class II-high and bear adsorbed *Xenopus* Igs. (A) FACS analysis of splenocytes from quiescent, adult *Xenpous*. Left panel shows MHC Class II by IgM, gated on leukocytes. Second panel shows light scatter profile of T cells, XL cells, and B cells, as gated in left panel. Right panels show CD5 expression and PNA binding of same subsets. (B) Analysis of splenocytes from day 9 post-immunization (PE/IFA) adult *Xenopus* was performed as in left panels in (A). Right panels show PE accumulation on XL cells and B cells, respectively. (C) Analysis of Ig adsorption on XL cells from day 16 post-immunization (PE/IFA) splenocytes. Left shows MHC Class II by PE, right panel shows IgY by IgM, gated on MHC II^{hi} PE^{+} population. Data are representative of at least 3 independent experiments, 2 animals per experiment. (D) Relative percentages of splenic B cells, T cells, and XL cells from either naïve ($n = 4$) or day 9 ($n = 6$) post-immunization animals, mean + SD shown, and obtained from 3 independent experiments with 1–2 animals per experiment. NS = not significant (by Student's *t*-test).

from immunized animals by in situ hybridization (ISH) for expression of FDC-associated genes (Fig. 2C). We detected expression of both the B cell chemoattractant CXCL13 and the B cell survival factor BAFF, both of which are expressed by mammalian FDC [22], in a pattern consistent with the repositioned XL cells at the internal perimeter of the WP. We also detected expression of a *cis*-duplicate of the polyIg receptor (pIgR) in *Xenopus*, tentatively named pIgR2 (manuscript in preparation). pIgR2 is capable of binding IgM and IgX (unpublished observations); we hypothesize that it is involved in immune complex (IC) acquisition by XL cells. Expression of both CXCL13 and pIgR2 by XL cells was confirmed by RT-PCR (see Fig. 4). Surprisingly, we were unable to detect CXCL13 in the naïve WP by ISH (Fig. 2D); CXCL13 mRNA, however, was detectable by semi-qRT-PCR analysis of total splenic RNA from naïve and immunized animals, and its levels increased following immunization (Fig. 2E). These data demonstrate that XL cells have FDC-like properties, including the capacity to both recruit and promote the survival of B cells, as well as to present

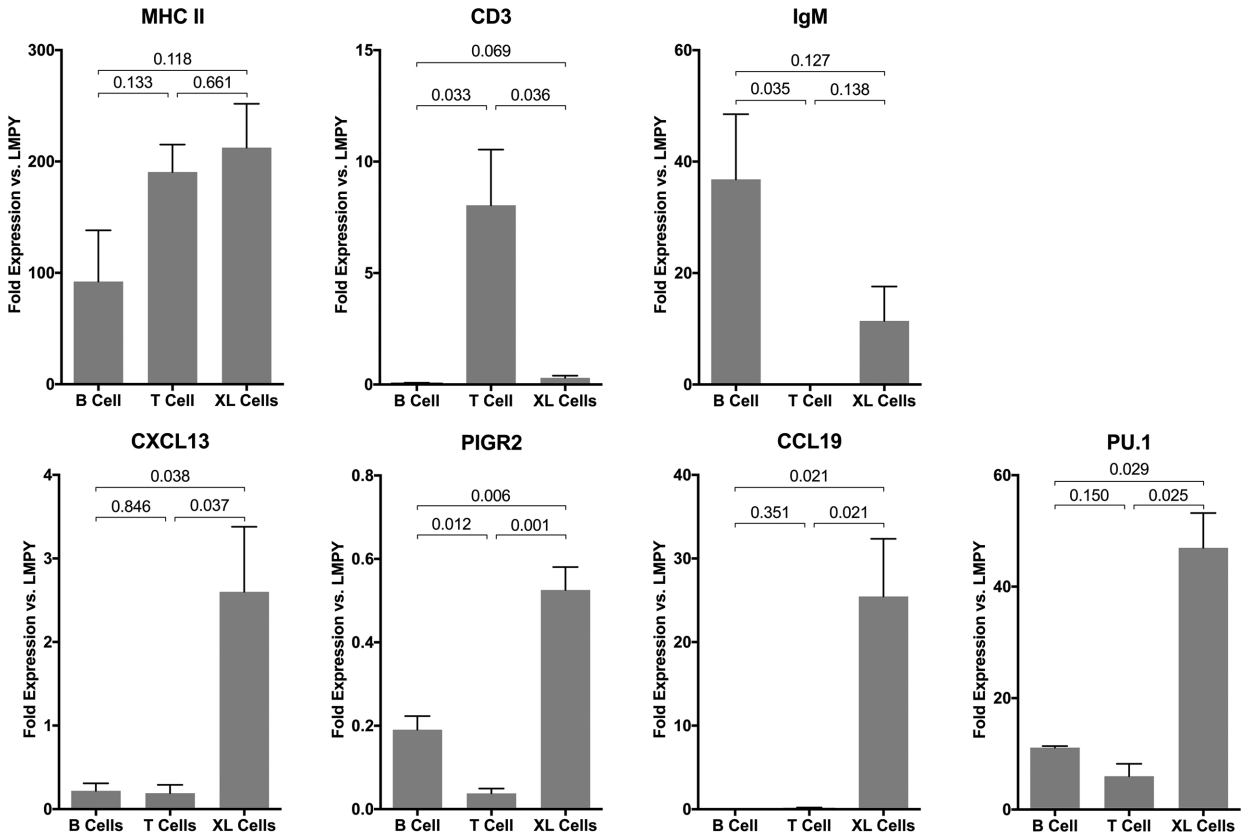

Figure 4. Gene expression profile of flow-sorted XL cells from immunized animals. Real-time qPCR analysis of CD3, IgM, MHC Class II, CXCL13, PIGR2, PU.1, and CCL19 expression in sorted B, T, and XL cells, relative to expression of the constitutive proteasomal subunit LMPY. Data are representative of 3 independent experiments, using 10 pooled spleens per experiment run in triplicate. Mean + SEM shown, P values generated by Student's *t*-test.

native antigen to B cells for clonal selection. These observations suggesting FDC-like functionality are intriguing, as our data suggest that XL cells are not bona fide FDC (see below), and FDC have not been definitively identified in any vertebrates other than mammals.

Identification of XL cells by FACS

The acquisition and retention of PE by XL cells provided a novel parameter by which these cells could be identified. Therefore, in order to further characterize the XL cells, we analyzed splenocytes from quiescent and day 9 post-immunization animals by flow cytometry, using mAbs specific for *Xenopus* MHC Class II [15], IgM [23], and CD5, the latter of which is constitutively expressed by *Xenopus* T cells [24]. In the quiescent spleen, three populations of MHC Class II$^+$ cells were observed: IgM$^+$/CD5$^-$/MHC Class II$^+$ B cells (approximately 22.2% of splenic leukocytes), IgM$^-$/CD5$^+$/MHC Class II$^+$ T cells (approximately 37.4% of splenic leukocytes; note that *Xenopus* T cells were shown previously to express class II at equivalent levels to B cells [15]), and a third population, representing approximately 2.0% of splenic leukocytes, of IgM$^{lo/-}$/CD5$^{lo/-}$/MHC Class II^{hi} cells with a high light scatter profile suggestive of the myelo-monocytic lineage (Fig. 3A, relative percentages of cells shown in Fig. 3D). Additionally, the latter population also stained positively with PNA (as did B cells), similar to cDC recently found in the teleost spleen [25].

After immunization (Fig. 3B, relative percentages of cells shown in Fig. 3D), we observed two distinct populations of PE+ cells: a very small proportion of PE$^+$ B cells, likely PE-reactive B cells, and a large proportion of the MHC Class II^{hi} population. The latter population also displayed increased levels of cell surface-associated IgM compared to those observed in quiescent animals. This increase in surface-associated IgM was also observed after immunization with HEL (Supporting Information Fig. 3), increasing by day 7 post-immunization and further increasing by day 14. While neither IgX nor IgY was detectable on the surface of XL cells from either quiescent or day 9 post-immunization animals, IgY, along with further elevated levels of IgM, was detected on day 16 post-immunization XL cells (Fig. 3C). This timeframe is consistent with Ag-driven CSR, suggesting that the surface acquisition of IgY is dependent upon IC formation, and possibly also mediated by an as yet undefined Fc and/or complement receptor.

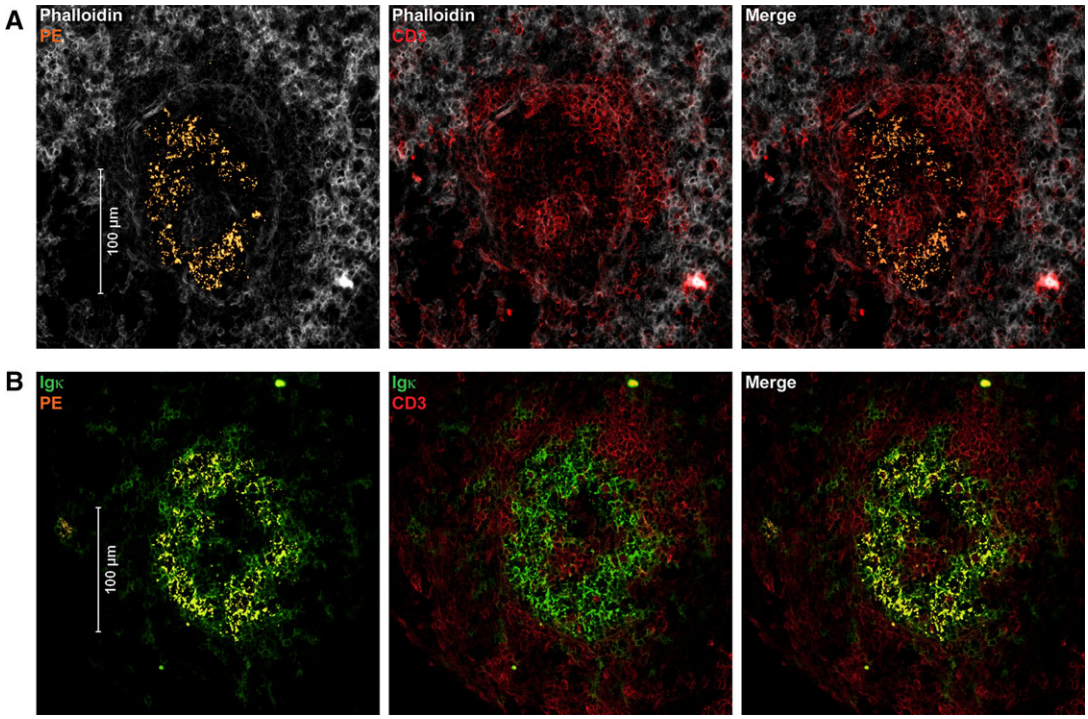

Figure 5. T cell immigration into the immunized WP. (A) representative image of a WP crypsection from a day 9 post-immunization (PE/IFA) spleen, stained with Phalloidin (white), anti-CD3 (red), and imaged for PE fluorescence (orange). (**B**) cryosection serial to section shown in (**A**), stained with anti-Igκ (green), anti-CD3 (red), and imaged for PE fluorescence (orange). Data are representative of at least 3 independent experiments on 1 animal per experiment, 3 animals in total. Magnification: 200×, scale bar: 100 μm.

XL cells as cDC

Predicting that the MHCII^{hi}, PE^{+} population comprised the XL cells we observed histologically in the immune WP, these putative XL cells were both MACS-sorted (Supporting Information Fig. 4) to confirm their morphology, and flow-sorted, along with B cells and T cells, for transcriptional analysis (sorting parameters in Supporting Information Fig. 5). The specificity of the sort was confirmed by analysis of MHC Class II, expressed by all three populations, and CD3, expressed by T cells but neither B cells nor XL cells (Fig. 4). IgM H chain mRNA was robustly detected in the B cell fraction but not in the T cell fraction, while a low level of expression was detected in the XL cell fraction, likely the result of a small amount of contamination of the sorted population by B cells (no reciprocal contamination of the B cell population was observed). Analysis of CXCL13 and pIgR2, both exclusively expressed by XL cells, confirmed the identity of the cells visualized by ISH in Fig. 2C.

Further analysis revealed expression of the hematopoietic transcription factor PU.1 by all three sorted populations, with significantly higher expression in the XL cells than in the lymphocyte populations; elevated expression of PU.1 compared to lymphocytes is characteristic of mammalian cDC, and its absence of expression in FDC [26]. Additionally, XL cells alone expressed the T cell chemoattractant CCL19. Coexpression of both MHC Class II and PU.1 demonstrates that the XL cells are of a conventional, hematopoietic lineage, and expression of CCL19 and MHC Class II suggest a cDC-like capacity to recruit and stimulate T cells, respectively. These data, when evaluated in concert with their surface retention of native Ag and expression of FDC-associated genes, suggest a dual functionality of XL cells, *i.e.* the capacity to act as APC for both T and B lymphocytes. Furthermore, the coordinated migration of XL cells into the B cell follicle in the context of an acute immune response suggests that their B cell-associated functions are central to their overall purpose.

T/B interface in the immune WP

As in mammals, *Xenopus* B cells express CXCR5, while T cells express CCR7 (unpublished observations). As such, the expression of CCL19 by XL cells from day 9 post-immunization spleen suggested an active recruitment of T cells into the WP during an acute immune response. Immunofluorescent analysis of splenic cryosections from immunized animals revealed high levels of T cell immigration into the WP, both at the internal perimeter and surrounding the central vasculature (Fig. 5A), suggesting recruitment of T cells both from the RP and from circulation; this differs significantly from the naïve WP from which T cells are largely, if not entirely, absent. (Fig. 1A).

Within the day 9 post-immunization WP, B cells were observed in intimate contact with PE-bearing XL cells (Fig. 5B). It should be noted that PE was detected on the surface of some B cells at day 9 post-immunization (see Fig. 3), and PE-bearing XL cells

also adsorb IgM – as such, the PE-bearing cells detected will likely contain both XL and B cells. Nevertheless, the XL cells are clearly distinguishable from the B cells by morphology, and represent the dominant population of PE-bearing cells at the internal perimeter of the WP. The immigrating T cells formed an interface with the WP B cells, at which T cell:B cell contact was observed. Notably, little if any direct T cell:XL cell contact was observed. This does not suggest, however, a lack of interaction between T cells and XL cells; the accumulation of Ag-bearing XL cells in the WP is a thymus-dependent event; as such, these data suggest a sequential interaction of XL cells with T cells prior to WP immigration, then with B cells (after WP immigration).

In mammals, T-dependent responses occur in 2 steps. B cells recognize native antigens in the follicle on FDC and become activated, modifying their chemokine receptors and moving to the edge of the follicle. T cells recognize antigen on cDC and move toward the follicular cxcl13 gradient, and also respond to chemokines made by the activated B cells like ccl3 and ccl4 that aid in their initiation of cognate interactions with B cells, which then either differentiate into plasma cells or form germinal centers. In a second step, T cells enter the follicles as T-follicular helper cells and interact with mutated/isotype-switched B cells at which point B cells either die, become memory cells, or differentiate into plasma cells.

In the case of DDDC, movement of antigen-laden APC into the follicle is T cell-dependent, likely a consequence of cognate interactions between antigen-specific T cells and the DDDC; subsequent contact between these 'licensed' DDDC with antigen-specific B cells might obviate the requirement for the first step in mammals; i.e. B cells might become activated, proliferate, and mutate/switch without direct T cell contact. We have noticed T cell movement into the follicle late in the response (likely in response to the CCL19 produced by XL cells post-immunization, and perhaps additional chemokines) and it seems likely that the 2nd step of the response in mammals, in which T cell interactions with B cells are required to preserve self tolerance and regulate the type of response made by B cells, is the evolutionarily older phase.

Discussion

The initiation of WP ontogeny, marked by perivascular B cell accumulation, is conserved from sharks to mammals [12–14]. Unlike in mammals, the B cell FO in both mature tadpole (beautifully visualized by Lametschwandtner *et* al, [27]) and adult *Xenopus* WP (as well as the mature WP in cartilaginous fish) is retained at the splenic vasculature. As such, retention of the B cell FO at the splenic vasculature represents the ancestral WP architecture; deviation from this conformation is only fully observed in mammals [1]. In mammals, detachment and migration from the vasculature is a characteristic of lymphotoxin (LT) a1b2-dependent pre-FDC maturation to FDC [16].

Nonetheless, canonical (*i.e.* AID-mediated (28), switch box-guided [28], T cell-dependent [29]) CSR occurs in the *Xenopus* spleen, as does SHM [30], and immunogen localization to the WP following thymus-dependent immunization has been reported [5]. These data suggest that the functions of FDC, if not the cells themselves, are conserved in *Xenopus*. SHM with limited affinity maturation occurs in all gnathostomes [31–33], so DDDC as defined here for *Xenopus* is likely the prototype for all cold-blooded vertebrates. Indeed, cells with similar morphological, functional, and migratory properties have been described in the spleen of the natterjack toad (*Bufo calamata*) [34, 35]). However, the precise microarchitecture of the spleen in *Xenopus*, in particular the compartmentalization of the WP from the RP, is not necessarily characteristic of all amphibia [36].

We have demonstrated that XL cells, the single established APC lineage in the *Xenopus* spleen, are of a conventional, hematopoietic lineage; whether these APC are macrophages that modify their phenotype after antigenic stimulation or DC derived from a dedicated precursor is not known, though previous data demonstrate that cells with the XL cell phenotype are functionally distinct from macrophages [8]. We have also demonstrated that XL cells are capable of retaining and therefore presenting native Ag at their plasma membrane, and are thus capable of performing the most central function of FDC. Their expression of CXCL13 and BAFF in the context of an acute immune response further supports their FDC-like function. It is not known at present why such an organized ring of DDDC forms in the FO; we suggest that a chemokine gradient originating either from the vasculature or GS orchestrates this conspicuous structure. Morphologically the PE-laden cells are definitely of the myeloid lineage (Supporting Information Fig. 4); future experiments will follow the XL cells over time at the morphological and expression levels.

LT alpha and beta are required for FDC formation and maintenance in mammals. While their absence in bony and cartilaginous fish is consistent with the lack of FDC in fish, amphibians clearly have both LT orthologues and yet also lack FDC. This dichotomy between fish and amphibians suggests that the latter have a more developed feature of antigen presentation to be defined. Perhaps LT plays a role in the migration of DDDC into the FO, which would be consistent with the thymectomy data (Supporting Information Fig. 2A [19]). Another possibility is that LT is involved in canonical CSR, which first appears in amphibians [37]. One last possibility is that the interaction with T cells through LT (or another way) might promote a conversion from cDC to FDC functionality by preventing antigen uptake or blocking acidification of lysosomes, both of which would preserve native antigen for presentation to B cells; this last possibility is consistent with the increase in surface antigen on DDDC after immunization, most likely in the form of immune complexes based both on the increase in IgM signal early after immunization (Fig. 3) and the subsequent acquisition of IgY. Note that these three possibilities are obviously not mutually exclusive.

Of note, these studies were performed using outbred *Xenopus;* the availability of isogeneic *Xenopus* will permit examination of all of these possibilities, especially the early functional interaction of

T cells with DDDC, as well as the functional interactions of DDDC with follicular B cells.

Materials and methods

Animals

Wild-type, outbred *Xenopus laevis* were bred in house under specific pathogen-free conditions or purchased from *Xenopus* Express, and housed at the University of Maryland. Larval developmental timepoints (from animals bred in-house) were determined by gross morphology. Adult, thymectomized J strain *Xenopus laevis* [38] and mock-surgery controls, were generated as described [39].

Immunizations

Adult *Xenopus* were immunized intraperitoneally with either 50 ug HEL (Sigma), suspended in amphibian PBS (aPBS) in Complete Freund's Adjuvant (Sigma) or 50 ug PE suspended in aPBS (Invitrogen) in Incomplete Freund's Adjuvant (Sigma). Animals were housed in 27C water post-immunization. Immunization in either CFA or IFA gave similar responses noted here. All procedures were approved by the UMB IACUC committees.

Immunohistochemistry (IHC)

Spleens were excised, immediately frozen in Tissue-Tek OCT Compound (Sakura), sectioned at 6uM on a CM3050S microtome (Leica), fixed for 30 s in ice-cold acetone, and stored at −80°C until staining. Thawed sections were blocked in 10% heat-inactivated horse serum in aPBS-T, and stained for 1 h. at 4°C with indicated antibody, then stained for 1 h at 4°C with secondary antibody, when applicable. Immunostained sections were analyzed on an Eclipse E800 microscope (Nikon) using a Spot RT3 camera (Diagnostic Instruments), and analyzed with Spot Advanced software. Images were adjusted for brightness and contrast using Adobe Photoshop Elements (Adobe Systems Inc.). Antibodies and stains are listed in Supporting Information Table 1.

Flow cytometry

Single cell suspensions of splenocytes were prepared by mechanical dissociation of spleen in aPBS + 2% FCS + 0.1% NaN3. Blood was collected by cardiac bleed, into aPBS + 10 U/mL heparin. Peritoneal cells were harvested by lavage in aPBS. Cells were stained with indicated antibody for 1 h on ice in aPBS (as appropriate) + 2% FCS + 0.1% NaN3, and acquired in PBS/aPBS + 0.1% NaN3 on an LSRII flow cytometer with FACS Diva software (BD Biosciences), and analyzed with FlowJo software (Tree Star). For sorting, single cell suspensions of *Xenopus* spleen were prepared and stained as above, then sorted on a FACS Aria II cell sorter (BD Biosciences) on 100 um nozzle at 20 psi sheath pressure and collected in aPBS + 2% FCS + NaN3. Antibodies and stains are listed in Supporting Information Table 1.

Magnetic cell separation

Single cell suspensions of splenocytes were prepared by mechanical dissociation of spleen in aPBS + 2% FCS + 0.1% NaN3, then mixed with anti-PE magnetic microbeads (Miltenyi). PE-bearing XL cells were magnetically separated, affixed to slides by cytospin, and stained with H&E.

In situ hybridization (ISH)

Spleens were excised and fixed O/N in 4% PFA at 4C, equilibrated in 30% sucrose, and frozen in Tissue-Tek OCT Compound (Sakura), then sectioned at 6uM on a CM3050S microtome (Leica) (38). In situ hybridization (ISH) was performed as previously described [40]. DIG-labeled probes were detected with anti-DIG_Alkaline Phosphatase (AP) and nitro-blue tetrazolium/5-bromo-4-chloro- 3′-indolyphosphate (NBT/BCIP) substrate. Oligo sequences used for riboprobe synthesis are listed in Supporting Information Table 1.

Quantitative PCR

Real-time quantitative PCR was performed on cDNA using the KiCqStart SYBR-Green Ready-Mix kit (Sigma, as per manufacturer's instructions) on a 7500 Fast DX Real-Time PCR Instrument (Applied Biosystems). Oligo sequences used for qPCR are listed in Supporting Information Table 1.

Acknowledgements: We thank Louis Du Pasquier for critical review of the manuscript, and Nevil Singh for helpful conversation and suggestions, as well as the *Xenopus laevis* Resource for Immunobiology (Rochester, NY, NIH R24 AI059830) for providing monoclonal Ab 2B1. This work was supported by National Institutes of Health Grant R01OD0549. H.R.N. was a trainee under Institutional Training Grant T32AI007540 from the National Institutes of Allergy and Infectious Diseases. H.R.N. performed most of the experimental work, including those from Figs. 1–5, S1–S3, and S5. J.G. contributed to the data from Figs. 3, S3, and S4. E.M.F. performed experimental work included in Fig. S4. M.F.C. provided thymectomized animals described in Fig. S3. H.R.N. and M.F.F. designed the

overall study, analyzed the data, and wrote the main body of the paper.

Conflict of interest: The authors declare no financial or commercial conflict of interest.

References

1 **Neely, H. R. and Flajnik, M. F.**, Emergence and evolution of secondary lymphoid organs. *Annu. Rev. Cell Dev. Biol.* 2016. **32**: 693–711.

2 **Boehm, T., Hess, I. and Swann, J. B.**, Evolution of lymphoid tissues. *Trends Immunol.* 2012. **33**: 315–321.

3 **Aguzzi, A., Kranich, J. and Krautler, N. J.**, Follicular dendritic cells: origin, phenotype, and function in health and disease. *Trends Immunol.* 2014. **35**: 105–113.

4 **Barreda, D. R., Neely, H. R. and Flajnik, M. F.**, Evolution of myeloid cells. *Microbiol Spectr* 2016. **4**: 45–58.

5 **Manning, M. J. and Horton, J. D.**, Histogenesis of lymphoid organs in larvae of the South African clawed toad, Xenopus laevis (Daudin). *J. Embryol. Exp. Morphol.* 1969. **22**: 265–277.

6 **Du Pasquier, L., Schwager, J. and Flajnik, M. F.**, The immune system of Xenopus. *Annu. Rev. Immunol.* 1989. **7**: 251–275.

7 **Baldwin, W. M., 3rd and Cohen, N.**, A giant cell with dendritic cell properties in spleens of the anuran amphibian Xenopus laevis. *Dev. Comp. Immunol.* 1981. **5**: 461–473.

8 **Turner, R. J.**, The functional development of the reticulo-endothelial system in the toad, Xenopus laevis (Daudin). *J. Exp. Zool.* 1969. **170**: 467–479.

9 **Leon, B., Ballesteros-Tato, A., Browning, J. L., Dunn, R., Randall, T. D. and Lund, F. E.**, Regulation of T(H)2 development by CXCR5+ dendritic cells and lymphotoxin-expressing B cells. *Nat. Immunol.* 2012. **13**: 681–690.

10 **Qi, H., Egen, J. G., Huang, A. Y. and Germain, R. N.**, Extrafollicular activation of lymph node B cells by antigen-bearing dendritic cells. *Science* 2006. **312**: 1672–1676.

11 **Grouard, G., Durand, I., Filgueira, L., Banchereau, J. and Liu, Y. J.**, Dendritic cells capable of stimulating T cells in germinal centres. *Nature* 1996. **384**: 364–367.

12 **Vondenhoff, M. F., Desanti, G. E., Cupedo, T., Bertrand, J. Y., Cumano, A., Kraal, G., Mebius, R. E. et al.**, Separation of splenic red and white pulp occurs before birth in a LTalphabeta-independent manner. *J. Leukoc. Biol.* 2008. **84**: 152–161.

13 **Neely, H. R. and Flajnik, M. F.**, CXCL13 responsiveness but not CXCR5 expression by late transitional B cells initiates splenic white pulp formation. *J. Immunol.* 2015. **194**: 2616–2623.

14 **Rumfelt, L. L., McKinney, E. C., Taylor, E. and Flajnik, M. F.**, The development of primary and secondary lymphoid tissues in the nurse shark Ginglymostoma cirratum: B-cell zones precede dendritic cell immigration and T-cell zone formation during ontogeny of the spleen. *Scand. J. Immunol.* 2002. **56**: 130–148.

15 **Du Pasquier, L. and Flajnik, M. F.**, Expression of MHC class II antigens during Xenopus development. *Dev. Immunol.* 1990. **1**: 85–95.

16 **Krautler, N. J., Kana, V., Kranich, J., Tian, Y., Perera, D., Lemm, D., Schwarz, P. et al.**, Follicular dendritic cells emerge from ubiquitous perivascular precursors. *Cell* 2012. **150**: 194–206.

17 **Du Pasquier, L., Robert, J., Courtet, M. and Mussmann, R.**, B-cell development in the amphibian Xenopus. *Immunol. Rev.* 2000. **175**: 201–213.

18 **Horton, J. D. and Manning, M. J.**, Lymphoid organ development in Xenopus thymectomized at eight days of age. *J. Morphol.* 1974. **143**: 385–396.

19 **Horton, J. D. and Manning, M. J.**, Effect of early thymectomy on the cellular changes occuring in the spleen of the clawed toad following administration of soluble antigen. *Immunology* 1974. **26**: 797–807.

20 **Phan, T. G., Grigorova, I., Okada, T. and Cyster, J. G.**, Subcapsular encounter and complement-dependent transport of immune complexes by lymph node B cells. *Nat. Immunol.* 2007. **8**: 992–1000.

21 **Phan, T. G., Green, J. A., Gray, E. E., Xu, Y. and Cyster, J. G.**, Immune complex relay by subcapsular sinus macrophages and noncognate B cells drives antibody affinity maturation. *Nat. Immunol.* 2009. **10**: 786–793.

22 **Rahman, Z. S., Rao, S. P., Kalled, S. L. and Manser, T.**, Normal induction but attenuated progression of germinal center responses in BAFF and BAFF-R signaling-deficient mice. *J. Exp. Med.* 2003. **198**: 1157–1169.

23 **Hsu, E. and Du Pasquier, L.**, Studies on Xenopus immunoglobulins using monoclonal antibodies. *Mol. Immunol.* 1984. **21**: 257–270.

24 **Jurgens, J. B., Gartland, L. A., Du Pasquier, L., Horton, J. D., Gobel, T. W. and Cooper, M. D.**, Identification of a candidate CD5 homologue in the amphibian Xenopus laevis. *J. Immunol.* 1995. **155**: 4218–4223.

25 **Lugo-Villarino, G., Balla, K. M., Stachura, D. L., Banuelos, K., Werneck, M. B. and Traver, D.**, Identification of dendritic antigen-presenting cells in the zebrafish. *Proc Natl Acad Sci U S A* 2010. **107**: 15850–15855.

26 **Carotta, S., Dakic, A., D'Amico, A., Pang, S. H., Greig, K. T., Nutt, S. L. and Wu, L.**, The transcription factor PU.1 controls dendritic cell development and Flt3 cytokine receptor expression in a dose-dependent manner. *Immunity* 2010. **32**: 628–641.

27 **Lametschwandtner, A., Radner, C. and Minnich, B.**, Microvascularization of the spleen in larval and adult Xenopus laevis: histomorphology and scanning electron microscopy of vascular corrosion casts. *J. Morphol.* 2016. **277**: 1559–1569.

28 **Zarrin, A. A., Alt, F. W., Chaudhuri, J., Stokes, N., Kaushal, D., Du Pasquier, L. and Tian, M.**, An evolutionarily conserved target motif for immunoglobulin class-switch recombination. *Nat. Immunol.* 2004. **5**: 1275–1281.

29 **Horton, J. D., Horton, T. L., Dzialo, R., Gravenor, I., Minter, R., Ritchie, P., Gartland, L. et al.**, T-cell and natural killer cell development in thymectomized Xenopus. *Immunol. Rev.* 1998. **166**: 245–258.

30 **Du Pasquier, L., Wilson, M., Greenberg, A. S. and Flajnik, M. F.**, Somatic mutation in ectothermic vertebrates: musings on selection and origins. *Curr. Top. Microbiol. Immunol.* 1998. **229**: 199–216.

31 **Hinds-Frey, K. R., Nishikata, H., Litman, R. T. and Litman, G. W.**, Somatic variation precedes extensive diversification of germline sequences and combinatorial joining in the evolution of immunoglobulin heavy chain diversity. *J. Exp. Med.* 1993. **178**: 815–824.

32 **Wilson, M., Hsu, E., Marcuz, A., Courtet, M., Du Pasquier, L. and Steinberg, C.**, What limits affinity maturation of antibodies in Xenopus–the rate of somatic mutation or the ability to select mutants? *EMBO J.* 1992. **11**: 4337–4347.

33 **Greenberg, A. S., Avila, D., Hughes, M., Hughes, A., McKinney, E. C. and Flajnik, M. F.**, A new antigen receptor gene family that undergoes rearrangement and extensive somatic diversification in sharks. *Nature* 1995. **374**: 168–173.

34 **Garcia Barrutia, M. S., Leceta, J., Fonfria, J., Garrido, E. and Zapata, A.**, Non-lymphoid cells of the anuran spleen: an ultrastructural study in the natterjack, Bufo calamita. *Am. J. Anat.* 1983. **167**: 83–94.

35 **Garcia Barrutia, M. S., Villena, A., Gomariz, R. P., Razquin, B. and Zapata, A.**, Ultrastructural changes in the spleen of the natterjack, Bufo calamita, after antigenic stimulation. *Cell Tissue Res.* 1985. **239**: 435–441.

36 **Zapata, A. and Amemiya, C. T.**, Phylogeny of lower vertebrates and their immunological structures. *Curr. Top. Microbiol. Immunol.* 2000. **248**: 67–107.

37 **Flajnik, M. F.**, Comparative analyses of immunoglobulin genes: surprises and portents. *Nat. Rev. Immunol.* 2002. **2**: 688–698.

38 **Tochinai, S., Nagata, S. and Katagiri, C.**, Restoration of immune responsiveness in early thymectomized xenopus by implantation of histocompatible adult thymus. *Eur. J. Immunol.* 1976. **6**: 711–714.

39 **Mashoof, S., Goodroe, A., Du, C. C., Eubanks, J. O., Jacobs, N., Steiner, J. M., Tizard, I. et al.**, Ancient T-independence of mucosal IgX/A: gut microbiota unaffected by larval thymectomy in Xenopus laevis. *Mucosal Immunol* 2013. **6**: 358–368.

40 **Criscitiello, M. F., Ohta, Y., Saltis, M., McKinney, E. C. and Flajnik, M. F.**, Evolutionarily conserved TCR binding sites, identification of T cells in primary lymphoid tissues, and surprising trans-rearrangements in nurse shark. *J. Immunol.* 2010. **184**: 6950–6960.

Abbreviations: **Ag**: Antigen · **APC**: Antigen Presenting Cell · **cDC**: Conventional Dendritic Cell · **CFA**: Complete Freund's Adjuvant · **CR**: Complement Receptor · **CSR**: Class Switch Recombination · **DC**: Dendritic Cell · **FDC**: Follicular Dendritic Cell · **FO**: Follicle · **GC**: Germinal Center · **GS**: Grenzschichtmembran of Sterba · **HEL**: Hen Egg Lysozyme · **IC**: Immune Complex · **IFA**: Incomplete Freund's Adjuvant · **Ig**: Immunoglobulin · **ISH**: in situ Hybridization · **LT**: Lymphotoxin · **MHC**: Major Histocompatibility Complex · **PALS**: Periarteriolar Lymphoid Sheath · **PE**: r-Phycoerythrin · **pIgR**: Poly-Ig Receptor · **RP**: Red Pulp · **SHM**: Somatic Hypermutation · **TCR**: T Cell Receptor · **TD**: Thymus-Dependent · **WP**: White Pulp

Full correspondence: Dr. Martin F. Flajnik, Department of Microbiology and Immunology, University of Maryland Baltimore, Suite 380, 685 West Baltimore St., Baltimore, MD 21201, USA
e-mail: mflajnik@som.umaryland.edu

See accompanying Commentary:
https://doi.org/10.1002/eji.201747459

Received: 2/8/2017
Revised: 20/10/2017
Accepted: 7/12/2017
Accepted article online: 12/12/2017

